

Article

# Effect of Al-B<sub>2</sub>O<sub>3</sub>-TiO<sub>2</sub> Exothermic System on Performances of Fly Ash Glass/Ceramic Composite Coating

Yajun An, Weiqiang Li \*, Li Zhu, Jingjing Lu and Xianyang Liu

School of Mechanical Engineering, Liaoning Technical University, Fuxin 123000, China; Anyajun\_01@163.com (Y.A.); 18341843257@163.com (L.Z.); 18341842637@163.com (J.L.); liuxianyang777@163.com (X.L.)

\* Correspondence: weiqiang\_777@163.com; Tel.: +86-183-4189-4459

Received: 3 December 2017; Accepted: 28 December 2017; Published: 16 January 2018

**Abstract:** Glass/ceramic composite coatings were prepared on 40Cr steel matrix by thermo-chemical reaction with fly ash and a small amount of SiO<sub>2</sub>, Al<sub>2</sub>O<sub>3</sub>, MgO, and albite as main raw materials. On this basis, adding 10% Al-TiO<sub>2</sub>-B<sub>2</sub>O<sub>3</sub> exothermic system, the morphology, phase, thermal shock resistance, and corrosion resistance of the coating were tested, and the influence of exothermic system on the structure and properties of the composite coating was studied. The experimental results show that the addition of exothermic system can promote the formation of NaB<sub>15</sub>, TiB<sub>2</sub>, Na<sub>2</sub>B<sub>4</sub>O<sub>7</sub>, Ca<sub>2</sub>Al<sub>2</sub>SiO<sub>7</sub>, and other new phases by thermo-chemical reaction; when compared to the composite coating without addition of exothermic system, combined with a good interface, higher compactness, and lower porosity. The highest micro hardness can be reached 725HV0.1. The number of thermal shock from 700 °C to room temperature can reach more than 50 times; acid, salt, oil immersion corrosion test, composite coating with exothermic system relative to the matrix increased by 27.40 times, 3.97 times, and 1.88 times, respectively. The overall performance is better than that of the composite coating without exothermic system.

**Keywords:** fly ash; 40Cr; exothermic system; properties analysis; thermal shock resistance

## 1. Introduction

Fly ash is industrial waste discharged from coal-burning in power plants, and now at an initial stage for China to make use of it. Traditionally, its application is distributed mainly in construction, agricultural production, and environmental treatment etc., but fly ash can actually bring higher added value [1–3]. Fly ash is mostly made up of ceramic phase and glass phase. It is viable to prepare glass-ceramic composite coating with fly ash as raw material [4–6].

Su H.L. et al. CaO-Al<sub>2</sub>O<sub>3</sub>-SiO<sub>2</sub> system fly ash glass ceramics were prepared by sintering method with fly ash as the main raw material [7]. Chen G.H. et al. Fly ash was used to prepare glass ceramics, and studied the amount of fly ash, its preparation process, and the determination of its performance. The results indicated that fly ash preparation of glass ceramics is viable [8]. The fly ash is properly treated, and then the fly ash is changed into waste, according to a certain process. The glass ceramics with high added value applied in building decoration are produced by Zhang J.Q. [9].

In practice, major forms of failure for machine elements are corrosion, wear, and fracture. Thus, it is crucial to improve wear resistance and corrosion resistance. Ceramics relative to steel is both high temperature and wear resistant, while glass relative to steel shows good corrosion resistance [4,5]. So, by combining these two materials and forming a compact glass-ceramic composite coating on the surface of steel will promote its corrosion-resistant performance. The method of thermo-chemical reaction is featured with simple process, low cost, and no special equipment is needed, and both

mechanical and chemical cohesion are existing between coating and the steel matrix [10]. In addition, the coating is easily controlled and strong in cohesion.

The corrosion of oil pipelines has occurred in all major oil fields. According to incomplete statistics, in recent years, about 80% of the failure of oil equipment is related to the corrosion of tubing. Each year, only the tubing corrosion can cause billions of dollars in loss, and it also brings serious environmental pollution. Because of the serious corrosion of the oil pipeline, it is imminent to carry out the research on the environmental corrosion behavior of the simulated petroleum medium [11–13].

The research status of thermo-chemical reaction ceramic coating is reviewed [14]. The fly ash composite coating with exothermic system were prepared on Q235 steel substrate by thermo-chemical reaction [15]. The erosion and wear properties of the composite coatings at different speeds and thermo-dynamic and dynamic analysis of the composite coatings were studied by Ma [16,17]. Li M. et al. studied the preparation of coating on metal surface by spraying and thermo-chemical reaction and the coating the properties of the coating were analyzed [18]. It is concluded from the experiment that the lower the porosity, the better the compactness and the higher the bonding strength of the coating to the interface.

This article is about preparing glass-ceramic coating on the 40Cr steel matrix, employing fly ash as raw material, with some additives added and the thermo-chemical reaction method is adopted. Following the introduction of a 10% Al-TiO<sub>2</sub>-B<sub>2</sub>O<sub>3</sub> exothermic system, its impact on the structure and performances of the composite coating is studied. The use of fly ash to prepare composite coating creates not only a new source of raw materials for preparing composite coating, but greatly reduce the cost of composite coating preparation, and also achieving the application with highly added value of fly ash itself. Thus, it is of great significance for both environmental pollution reduction, energy conservation, and sustainable development.

Glass-ceramic composite coatings are widely used in aerospace, biomedicine, decoration materials, and other fields because of their high strength, good chemical stability, good wear resistance, and corrosion resistance [19–23]. Its application will be more extensive in the future.

## 2. Test Materials and Method

### 2.1. Test Materials and Preparation of Coating

In this test, 40Cr steel (for its chemical composition, see Table 1) is adopted as matrix with its specifications 20 mm × 20 mm × 3.5 mm. First of all, apply mechanical sanding onto the steel matrix to get rid of oxide skin, so the test sample can get activated and coarsened. Therefore, the coarsened surface increases the contact area between the coating and steel matrix and helps promote the bond strength between them. Then, spray on the steel matrix surface the Ni-Al powdered alloy as transition layer following the process of pre-treatment, such as acetone cleaning, etc. to alleviate cracking, exfoliation resulting from discrepancy of thermal expansion between coating and matrix.

**Table 1.** The chemical composition of 40Cr steel (wt %).

| C         | Si        | Mn        | S      | P      | Cr        | Ni     | Cu     |
|-----------|-----------|-----------|--------|--------|-----------|--------|--------|
| 0.37–0.44 | 0.17–0.37 | 0.50–0.80 | ≤0.035 | ≤0.035 | 0.80–1.10 | ≤0.030 | ≤0.030 |

The fly ash that was discharged from Fuxin Power Plant is chosen as main raw material (the composition is determined by the Northeast mineral resources supervision and detection center of the Ministry of land and resources, see Table 2). Other ingredients are also added with a ratio SiO<sub>2</sub>:Al<sub>2</sub>O<sub>3</sub>:MgO:albite = 67:22:5:5 for proportioning and weighing. To study effect of the exothermic system on the performance of the composite coating, a 10% Al-TiO<sub>2</sub>-B<sub>2</sub>O<sub>3</sub> system is introduced into them and the same treatment process is adopted to prepare composite coating [24]. Al, when compared with TiO<sub>2</sub>, B<sub>2</sub>O<sub>3</sub>, has a better reducibility and is easier to react with refractory

oxide; while, Al powder has lower melting point, and is quicker to melt when reacting to fill air holes inside the coating, and release large amounts of heat, acting as thermite, which will further conduct chemical reaction. The reaction equation:  $10\text{Al} + 3\text{TiO}_2 + 3\text{B}_2\text{O}_3 = 5\text{Al}_2\text{O}_3 + 3\text{TiB}_2$ , the Gibbs free energy in the reaction  $\Delta G_T = -2847.65077 + 0.46256T$ . The release of this part of energy also helps to speed the thermal chemical reaction. The newly generated phases in the reaction, such as  $\text{Al}_2\text{O}_3$ ,  $\text{TiB}_2$  have good properties and help promote the performances of coating.  $\text{Al}_2\text{O}_3$  is a neutral oxide and corrosion-resistant to majority of solvents, like acid and salt etc., and with excellent performance resisting to corrosion.  $\text{TiB}_2$  is the most stable chemical compound combined by Boron and Titanium, with a melting point up to  $3225\text{ }^\circ\text{C}$  and also resistant to wear, corrosion, thermal shock, and anti-oxidation.

**Table 2.** The Chemical composition of fly ash (wt %).

| $\text{SiO}_2$ | $\text{Al}_2\text{O}_3$ | $\text{TFe}_2\text{O}_3$ | $\text{CaO}$ | $\text{K}_2\text{O}$ | $\text{MgO}$ | $\text{Na}_2\text{O}$ | $\text{TiO}_2$ | $\text{P}_2\text{O}_5$ | $\text{MnO}$ | Others |
|----------------|-------------------------|--------------------------|--------------|----------------------|--------------|-----------------------|----------------|------------------------|--------------|--------|
| 59.82          | 17.32                   | 8.23                     | 3.64         | 2.75                 | 2.61         | 1.37                  | 0.79           | 0.26                   | 0.11         | 3.10   |

Put two aggregates into the FS-150 ultrasonic crusher and crush for 1 h. After 8 h of ball-milling in the planetary-type QM-1SP2 ball grinder (Nanjing University Instrument Factory, Nanjing, China) at the speed of 400 r/min, the powders are sifted out through 200 mesh sieve and are uniformly blended with the inorganic agglomerate  $\text{Al}(\text{H}_2\text{PO}_4)_3$  at the ratio of 1.5:1; then put them into the JB-3 type (Beijing Tian Lian harmonious instrument and Instrument Ltd., Beijing, China) timing constant-temperature magnetic stirrer for preparing slurry which is applied to the after-pretreatment surface of the steel matrix by brush-painting uniformly. The thickness of the slurry on the matrix is not more than 1 mm. The sample is dried at room temperature for 24 h in the shade. The test sample is then placed in the GSL-1400 type vacuum furnace (Changzhou Xing Guang kiln Ltd., Changzhou, China) and slowly heated to  $950\text{ }^\circ\text{C}$  for thermo-curing. After thermal curing, heat treatment was carried out to obtain good mechanical properties of the base steel. The thermo-curing process is shown in Figure 1.

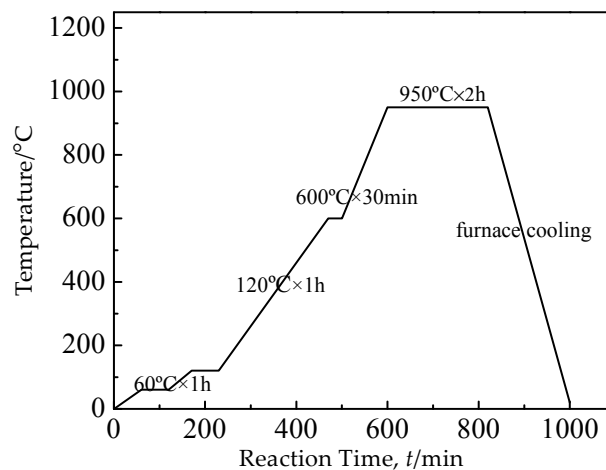


**Figure 1.** Thermo-curing process of coatings.

During the thermo-curing, the speed of increasing the temperature must be slow. The temperature rise is kept at about  $1\text{ }^\circ\text{C}/\text{min}$  before reaching  $120\text{ }^\circ\text{C}$ , especially at the low temperature stage; temperature must be fixed for 1 h at  $60\text{ }^\circ\text{C}$  and  $120\text{ }^\circ\text{C}$  each to get the water evaporated fully, so as to prevent such defects as swelling and air holes that are caused by rapidly increasing temperature in the process of thermo-curing [25].

## 2.2. Testing Methods for the Surface Features and Performance of Coating

Using the Hitachi SSX-550 (Shimadzu, Japan) type scanning electron microscope (SEM) to observe the cross-sectional features and interface bonding of these two kinds of composite coatings.

Adopting Rigaku's 2RIGAKU2500/PC type X-ray diffractometer (Akishima-shi, Japan) to carry out phase analysis of two kinds of coatings. Scanning speed: 8°/min, scanning scope: 10°–80°.

The coating is placed in the SX2-8-10 type mid-temperature resistor furnace (Shanghai Wei xing furnace industry Ltd., Shanghai, China) to heat until 700 °C, keeping 10 min. Then, quickly take out the sample and put into water to rapidly cool. After cooling, check and record whether or not cracks or exfoliation emerge. If none of them appears, it is considered one thermal shock cycle; then, put again the sample into the furnace to heat and repeat the cycle until the coating's area of cracks or exfoliation reach more than one-third of the overall area. This method can be used to determine the thermal shock resistance.

Static soaking is a major method to test the corrosion performance of material. The corrosion reagent chosen in this static corrosion test is 15% H<sub>2</sub>SO<sub>4</sub> solution, 3.5% NaCl, as well as self-made corrosive liquid with petroleum medium (for petroleum medium composition, see Table 3). To accurately test corrosion resistant performance of the composite coating in corrosive liquid, the working surface of the sample must be sealed with epoxy resin prior to the test, then seal coating holes with varnish. Next, begin the test by putting the coating into the corrosive liquid and keep static-soaking for a period of time, take out the sample, and wash with large amount of clean water and dry. At last, weigh the sample using FA100-4 type electronic balance (Wuhan gelaimo detection equipment Ltd., Wuhan, China) and calculate the sample's per-unit—area corrosion amount.

**Table 3.** Solute's amount of substance in 1 L solution/10<sup>−3</sup> mol.

| CaCl <sub>2</sub> | MgCl <sub>2</sub> | NaHCO <sub>3</sub> | NaSO <sub>4</sub> | NaCl   | KCl    |
|-------------------|-------------------|--------------------|-------------------|--------|--------|
| 7.515             | 4.558             | 1.800              | 1.751             | 61.998 | 68.640 |

## 3. Test Results and Analysis

### 3.1. Analysis of Cross-Sectional Features of Composite Coating

Figure 2 shows the cross-sectional features of composite coating before and after introduction of exothermic system. From top to bottom in the figure are, in order, coatings, intermediate layer, and matrix. The average thickness of the coating is 100 μm. For pre-introduction, the composite coating and transition layer are embedded each other and fused irregularly with interface still clearly visible; inside the coating are many cracks and small pores; the structure is relatively loose and poorly compact. For post-introduction, interface between composite coating and transition layer is blurred, coating and layer are more uniform and compact, and with fewer cracks and pores. Because introduction of exothermic system brings about the release of more heat, which makes thermo-chemical reaction going thoroughly and the coating and transition layer permeate fully and fuse together. Meanwhile, Al powder and B<sub>2</sub>O<sub>3</sub> in the exothermic system would be fused as liquid phases at temperatures of 660 °C and 450 °C, respectively, which spread uniformly and fill into cracks and pores inside the coating, greatly lower porosity. Therefore, a composite coating with more compact structure and better interface bonding can be acquired.

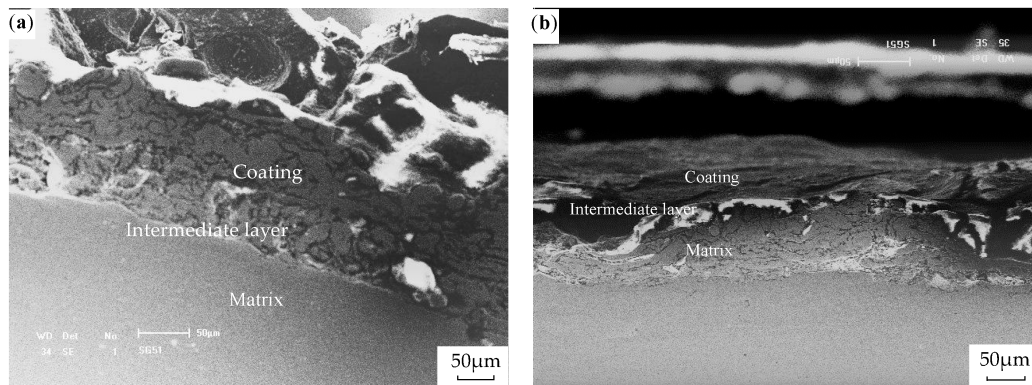


**Figure 2.** Scanning electron microscope (SEM) images of the composite coating (a) Coating without exothermic system; (b) Coating with exothermic system.

### 3.2. Phase Analysis of Composite Coating

Figures 3 and 4 show, respectively, the XRD of composite coatings before and after exothermic system is added. After coating thermo-curing at 950 °C, the pre-introduction of exothermic system coating generates new phases like  $\text{Ca}_2\text{Al}_2\text{SiO}_7$ ,  $\text{AlPO}_4$ ,  $\text{FeAl}_{13}$ ,  $\text{Mg}_3(\text{PO}_4)_2$ , etc.; the post-introduction coating produces fresh phases such as  $\text{Al}_6\text{O}_{13}\text{Si}_2$ ,  $\text{Na}_2\text{B}_4\text{O}_7$ ,  $\text{TiB}_2$ ,  $\text{NaB}_{15}$ ,  $\text{Al}_2\text{O}_3$ , etc. This indicates that whether exothermic system is added or not, the thermal chemical reactions could happen to composite coatings. Both Figures 3 and 4 show obviously broadened hilly-shaped diffraction peaks, which indicate amorphous substances or incomplete micro crystals, i.e., glass phase structure, appear, together with mullite phase, constituting the glass-ceramic composite coating. Meanwhile, the generation of new phases illustrates not only the mechanical combination, but also the chemical bonding in the process of thermo-chemical reaction that can greatly improve the coating's bonding strength. But, composite coating with exothermic system produces more new phases and one of which is hard phase  $\text{TiB}_2$  with a high melting point [26,27]; other new phases, such as  $\text{AlPO}_4$ ,  $\text{MgAl}_2\text{O}_4$ , and  $\text{Al}_6\text{O}_{13}\text{Si}_2$  are featured with excellent wear- and corrosion-resistance. Thus, its stability get dramatically improved.

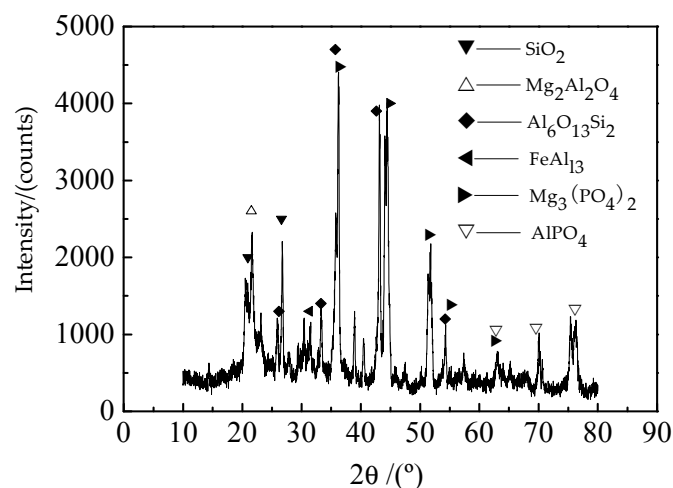


**Figure 3.** Composite coating without exothermic system.

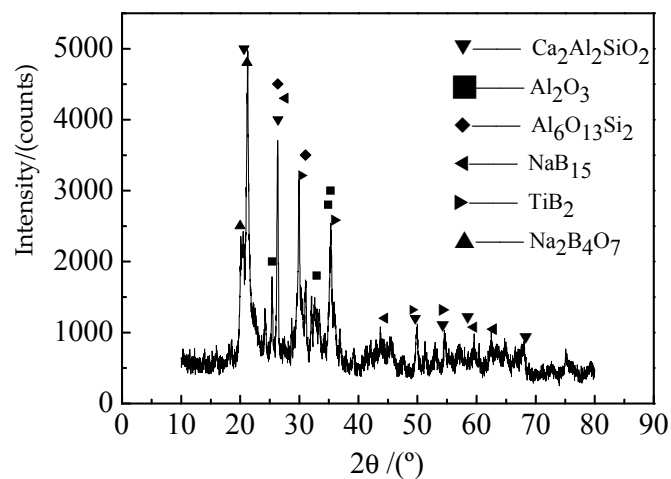


Figure 4. Composite coating with exothermic system.

### 3.3. Thermal Shock Resistance of Composite Coating

Thermal shock resistance refers to the ability for coating to resist dramatic temperature change and remain undamaged, and also is important indicator to evaluate coating's cohesive strength and bonding strength [28,29]. Thermal shock experimental data of two kinds of coatings are shown in Table 4.

Table 4. Thermal shock experimental data.

| Sample    | Cracking Frequency | Thermal Shock Frequency | Thermal Shock Phenomenon  |
|-----------|--------------------|-------------------------|---|
| Coating A | 17                 | 50                      | The crack at the edge of the coating starts to crack. With the increase of thermal shock times, there are small cracks on the surface. There are massive exfoliation on the edges, and the area of the shedding is increasing. The total area of the coating reaches 1/3 at fiftieth times. |
| Coating B | 35                 | More than 50            | When the number of thermal shock is 35 times, a small number of cracks begin to appear. When the number of thermal shock reaches 50 times, the coating still has no obvious falling off phenomenon. (stop experiment)   |

For thermal shocking at 700 °C, pre-introduction of exothermic system (A), composite coating gets to fall off following 17 thermal shock cycles. The exfoliation area, relative to the overall area of coating, approaches one-third after number of thermal shocks reaches 50. In contrast, post-introduction of exothermic system (B), composite coating starts to grow a few cracks; with 50 thermal shocks, coating shows no obvious fall-off. This is because the introduction of exothermic system can further promote chemical reaction and bring more glass and ceramic phases, which make structure inside the coating more uniformly distributed, reduce the differences of density, and expansion coefficient between coating phase and steel matrix. Thus, such composite coating with well-bonded interface and more compact structure is achieved.

### 3.4. Micro Hardness of Composite Coating

The micro hardness of coating is the ability of coating to resist deformation that is caused by external pressure, and is closely related to coating material, phase structure, interface bonding strength and compactness [30,31]. Can be seen from Figure 5, figure line level as the matrix hardness is about 170HV0.1, the maximum hardness of the composite coating without exothermic system is about

575HV0.1, relative to the hardness of the matrix increased 3.38 times. The maximum hardness of the composite coating with exothermic system is about 725HV0.1, relative to the hardness of the matrix increased 4.26 times and increased by about 150HV0.1 than the hardness of coating A.

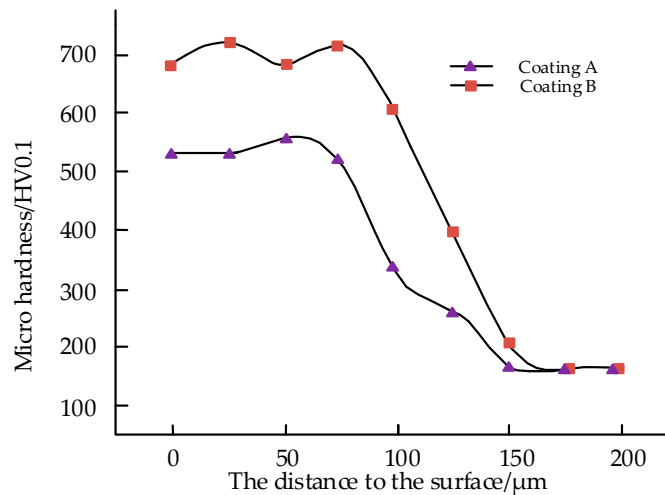


**Figure 5.** Micro hardness distribution curves of different coatings from fly ash along depth direction.

In addition, the micro hardness of the middle and upper part of coating B is higher than that of the middle and lower parts. This may be the reason that the content of hard phase, such as  $\text{Al}_2\text{O}_3$  and  $\text{TiB}_2$  in the coating, is high, while the middle and lower part is the transition zone between coating and alloy layer, so the micro hardness decreases. It is proved that the compactness and interface bonding strength of the coated B are better than that of the coating A.

### 3.5. Corrosion Resistance of Composite Coating

Table 5 shows the corrosion resistance data of matrix and composite coating soaked in 15%  $\text{H}_2\text{SO}_4$  solution (the corrosion data images of 15%  $\text{H}_2\text{SO}_4$  in solution, see Figure 6). Drown from the table, acid resistance, relative to steel matrix, of pre-introduction of exothermic system composite coating A, and post-introduction of exothermic system composite coating B increases by 17.8 times and 27.40 times, respectively. Factors to influence acid resistance of coating include coating's phase composition, compactness, and bonding strength etc. Fly ash contains large amount of  $\text{SiO}_2$  and  $\text{Al}_2\text{O}_3$ , and  $\text{SiO}_2$  with excellent acid resistant property to any acid except hydrofluoric acid. In addition, the introduction of albite helps generate new phases, one of which, the ceramic phase, can stably exist in acid;  $\text{Mg}_3(\text{PO}_4)_2$  has stronger acid resistance; the new phase  $\text{Ca}_2\text{Al}_2\text{SiO}_7$ , produced in the thermo-chemical reaction, is excellent in acid resistance and conducive to acid corrosion resistance of coating. Composite coating with the addition of exothermic system receives a more compact structure, well-distributed texture, and more kinds of new phases and lower porosity. Therefore, coating soaked longtime in corrosion is not easily corroded following the break-off or acid-corrosive fluid seeping inside down the pores and cracks. Thus, it shows better acid-resistance.

**Table 5.** The corrosion data of 15%  $\text{H}_2\text{SO}_4$  in solution.

| Sample    | Loss of Weight per Unit Area/ $\text{g}\cdot\text{m}^{-2}$ |         |         |         |          |          |          | Relative Corrosion Resistance |
|-----------|--|---------|---------|---------|----------|----------|----------|-------------------------------|
|           | 4 h  | 8 h     | 12 h    | 16 h    | 20 h     | 24 h     | 36 h     |                               |
| Matrix    | 16.5501  | 44.0311 | 52.7912 | 94.3612 | 107.5723 | 141.7943 | 281.0500 | 1.00                          |
| Coating A | 3.4101   | 3.5021  | 6.6709  | 6.7415  | 6.8901   | 7.1203   | 7.7211   | 17.80                         |
| Coating B | 0.7681   | 1.6422  | 2.9332  | 4.0323  | 4.6412   | 4.7731   | 5.0650   | 27.40                         |

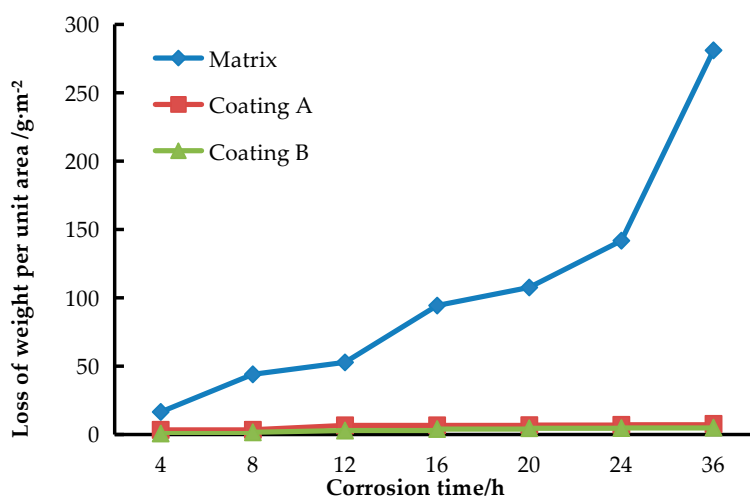


Figure 6. The corrosion data images of 15% H<sub>2</sub>SO<sub>4</sub> in solution.

Table 6 presents corrosion data for composite coating soaked in 3.5% NaCl solution, which shows salt resistance of composite coatings without exothermic system and composite coatings with exothermic system, relative to matrix, increases by 1.31 times and 3.97 times, respectively. (The corrosion data images of 3.5% NaCl in solution, see Figure 7). The corrosion mechanism of NaCl is mainly because that tiny-radius Cl<sup>-</sup> permeates into the coating through its thorough-holes and blind holes, and causes corrosion. However, composite coating during thermo-chemical reaction would certainly bring about air holes, through which tiny-radius Cl<sup>-</sup> easily permeates into transition layer or matrix and causes corrosion if exothermic system is not added, so the coating shows limited ability to resist salt corrosion. After the introduction of exothermic system, composite coating can undergo thermo-chemical reaction with a greater extent, making low-melting-point albite melt and fill pores inside coating, so the coating gets more compact; such hard and glass phases as Na<sub>2</sub>B<sub>4</sub>O<sub>7</sub>, TiB<sub>2</sub>, NaB<sub>15</sub> and Ca<sub>2</sub>Al<sub>2</sub>SiO<sub>7</sub> are generated inside coating, the complex lattice structure slows down permeation speed of chemical factors. Therefore, composite coating acquires a better salt resistance after the introduction of exothermic system.

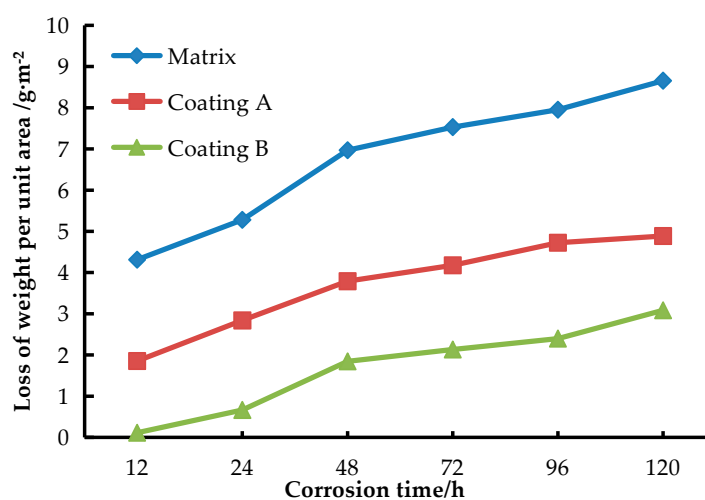


Figure 7. The corrosion data images of 3.5% NaCl in solution.

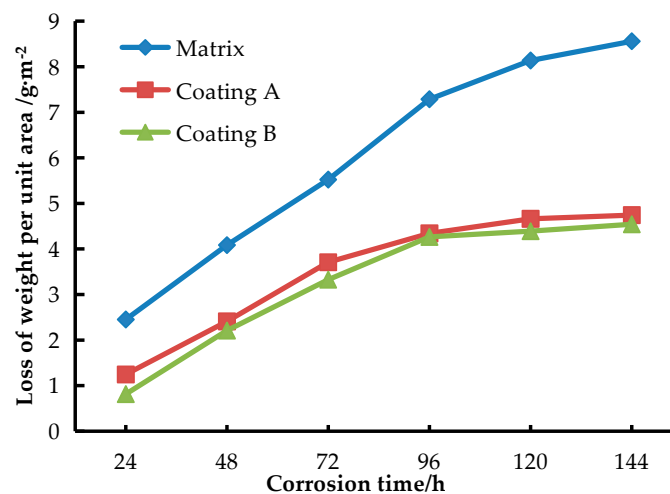
**Table 6.** The corrosion data of 3.5% NaCl in solution.

| Sample    | Loss of Weight per Unit Area/ $\text{g}\cdot\text{m}^{-2}$ |        |        |        |        |        | Relative Corrosion Resistance |
|-----------|--|--------|--------|--------|--------|--------|-------------------------------|
|           | 12 h   | 24 h   | 48 h   | 72 h   | 96 h   | 120 h  |                               |
| Matrix    | 4.3125   | 5.2812 | 6.9688 | 7.5313 | 7.9516 | 8.6579 | 1.00                          |
| Coating A | 1.8548   | 2.8387 | 3.7903 | 4.1774 | 4.7258 | 4.8871 | 1.31                          |
| Coating B | 0.1142   | 0.6664 | 1.8468 | 2.1324 | 2.3990 | 3.0844 | 3.97                          |

Corrosion data is presented in Table 7 for matrix and coating soaked in petroleum medium (The corrosion data images of Petroleum medium, see Figure 8). In this test, a self-made petroleum medium is used as corrosive fluid and corrosion behavior of composite coating is simulated in the environment of petroleum medium. Many kinds of solutes are contained in petroleum medium, which leads to a more complicated corrosion environment. As seen from Table 7, corrosion resistance in petroleum medium pre- and post-introduction of exothermic system, relative to matrix, increases by 1.72 times and 1.88 times, respectively. At the initial stage of corrosion, surface of composite coating shows itself as glass state, effectively holding back chemical corrosion of the petroleum medium. Since it is inevitable for cracks to emerge during the preparation of coating when thermo-chemical reaction method is applied, inside and outside these cracks, concentration difference of oxygen appears. Thus, cells of oxygen concentration difference are formed, which leads to corrosion at cracks further aggravating. After certain period of time, glass phase starts to get damaged locally, the corrosive liquid constantly permeates down the pores and cracks in coating, and finally expands to transition layer or matrix interface, leading to grave corrosion. With the introduction of exothermic system, composite coating shows lower porosity, and reduces occurrence of corrosion to a certain extent, therefore it reveals better corrosion resistant performance in the petroleum medium corrosion [32].

**Table 7.** The corrosion data of Petroleum medium.

| Sample    | Loss of Weight per Unit Area/ $\text{g}\cdot\text{m}^{-2}$ |        |        |        |        |        | Relative Corrosion Resistance |
|-----------|--|--------|--------|--------|--------|--------|-------------------------------|
|           | 24 h   | 48 h   | 72 h   | 96 h   | 120 h  | 144 h  |                               |
| Matrix    | 2.4505   | 4.0842 | 5.5217 | 7.2861 | 8.1361 | 8.5603 | 1.00                          |
| Coating A | 1.2451   | 2.4110 | 3.7081 | 4.3432 | 4.6612 | 4.7416 | 1.72                          |
| Coating B | 0.8159   | 2.2088 | 3.3283 | 4.2663 | 4.3899 | 4.5412 | 1.88                          |

**Figure 8.** The corrosion data images of Petroleum medium.

#### 4. Conclusions

It is viable to prepare glass/ceramic composite coating on 40Cr steel with fly ash as main raw material, and with introduction of 10% Al-TiO<sub>2</sub>-B<sub>2</sub>O<sub>3</sub> exothermic system and an adoption of thermo-chemical reaction method, which enhances corrosion resistant performance of composite coating.

It can be drawn from an analysis of features and phases of coating, when thermo-curing at 950 °C, new phases like Ca<sub>2</sub>Al<sub>2</sub>SiO<sub>7</sub>, Na<sub>2</sub>B<sub>4</sub>O<sub>7</sub>, TiB<sub>2</sub>, and NaB<sub>15</sub> etc. are generated in composite coating. The highest micro hardness of the coating B can be reached 725HV0.1. Therefore, the coating B has good compactness, lower porosity, and better interfacial bonding performance than the coating A.

When soaked to corrode inside the 15% H<sub>2</sub>SO<sub>4</sub> solution, 3.5% NaCl solution and solution of petroleum medium, corrosion resistance of composite coating, excluding the introduction of exothermic system, relative to matrix, increases by 17.8 times, 1.31 times, and 1.72 times, respectively; in contrast, corrosion resistance of composite coating including introduction of exothermic system, relative to matrix, increases by 27.4 times, 3.97 times, and 1.88 times, respectively. Generally, it outperforms composite coating without introduction of exothermic system.

**Acknowledgments:** This work is supported by the National Natural Science Fund of China (U1261123) and the Science and technology research project of Liaoning Provincial Education Department (Lj2017faL010).

**Author Contributions:** Yajun An and Weiqiang Li conceived and designed the experiments; Weiqiang Li performed the experiments; Li Zhu and Jingjing Lu analyzed the data; Xianyang Liu contributed reagents/materials/analysis tools; Weiqiang Li wrote the paper.

**Conflicts of Interest:** The authors declare no conflict of interest.

#### References

1. Oriol, F.; Xavier, Q.; Roberto, J. Recovery of gallium and vanadium from gasification fly ash. *J. Hazard. Mater.* **2007**, *139*, 413–423.
2. Diaz, A.R.; Naoki, H.; Mayumi, I.; Masami, T. Recovery of heavy metals from MSW molten fly ash by CIP method. *Hydrometallurgy* **2009**, *97*, 8–14.
3. Mishra, S.C.; Mishra, P.C.; Rout, K.C.; Anantapadmanabahn, P.V. Fly ash as a coating material for plasma spray coatings. In Proceedings of the National Seminar on Fly Ash Utilisation, NML Jamshedpur, India, 26–27 February 1999; pp. 131–135.
4. Ke, W.; Yang, W. *Application and Failure Cases of Corrosion Science and Technology*; Chemical Industry Press: Beijing, China, 2006. (In Chinese)
5. Shen, C.J.; Liu, W.W.; Wang, F.S.; Yang, C.M. The performance of corrosion and abrasion of high velocity oxygen fuel spray 316L stainless steel coating on mine shaft steel guide. *J. China Coal Soc.* **2009**, *34*, 1713–1717. (In Chinese)
6. Zhou, J.E.; Li, J.K.; Jiang, W.H. Ceramic coatings preparation, application and developing direction to metallic-matrix. *J. Ceram.* **2004**, *25*, 179–185. (In Chinese)
7. Su, H.L.; Wang, L.J.; Wang, Z.S. Experimental study on preparation technology of CAS system fly ash glass-ceramics. *J. Funct. Mater.* **2011**, *42*, 1342–1345. (In Chinese)
8. Chen, G.H.; Zhao, S.X.; Yang, G.B. Application of fly ash in glass ceramics. *Fly Ash Compr. Util.* **1997**, *1*, 23–25. (In Chinese)
9. Zhang, J.Q. The Manufacture of Neo-ceramic Glass for Building Decoration with Fly Ash. *Coal Ash China* **2004**, *2*, 47–48. (In Chinese)
10. Feng, C.F.; Froyen, L. On the reaction mechanism of an Al-TiO<sub>2</sub>-B system for producing in situ (Al<sub>2</sub>O<sub>3</sub>-TiB<sub>2</sub>)/Al composites. *Scr. Mater.* **1998**, *39*, 109–118. [[CrossRef](#)]
11. Sun, J.; Geng, C.L.; Zhang, Z.T.; Wang, X.T.; Xu, L. Present situation of comprehensive utilization technology of industrial solid waste. *Mater. Rev.* **2012**, *26*, 105–109.
12. Li, S.H.; Zhu, Y.X. Corrosion protection of underground oil pipe. *Oil-Gas Field Surf. Eng.* **2007**, *26*, 45–56. (In Chinese) [[CrossRef](#)]

13. Liu, Z.Y.; Dong, C.F.; Li, X.G.; Tan, H.Q.; Yan, J.Q. Failure Analysis of API Oil Casing. *J. Iron Steel Res.* **2008**, *20*, 58–62.
14. Ma, Z.; Li, J.; Yan, C.J.; Li, Z.C. Preparation and Properties of Glass-ceramic Composite Coating from Fly Ash. *Bull. Chin. Ceram. Soc.* **2013**, *32*, 1684–1687. (In Chinese)
15. Ma, Z.; Tao, Y.; Li, Z.C. Forecast on Fly Ash Ceramic Coatings by Thermal Chemical Reaction. *Bull. Chin. Ceram. Soc.* **2012**, *31*, 27–31. (In Chinese)
16. Ma, Z.; Ji, X.W.; Li, P.; Dong, S.Z.; Li, Z.C. Thermo-dynamics and Kinetics Analysis of Composite Ceramic Coatings Al-TiO<sub>2</sub>-B<sub>2</sub>O<sub>3</sub> System. *Bull. Chin. Ceram. Soc.* **2010**, *29*, 582–587. (In Chinese)
17. Ma, Z.; Tao, Y.; Yang, J.; Zhou, P.; Li, Z.C. Effect of Exothermic Chemical System on Corrosion Resistance of Glass-ceramic Composite Coatings from Fly Ash. *Bull. Chin. Ceram. Soc.* **2014**, *33*, 1609–1613. (In Chinese)
18. Li, M.; Liu, J.R.; Huang, W.D. The Properties of Spraying and Thermo-chemical Reaction Coating on the Metal Mold Surface. *Foundry* **2014**, *63*, 523–527. (In Chinese)
19. Grossman, D.G. Machinable glass-ceramics based on tetra silicic mica. *J. Am. Ceram. Soc.* **1972**, *55*, 446–449. [[CrossRef](#)]
20. Xia, A.; Miao, H.Y. Study and preparation of composites of Y-TZP/mica-based glass-ceramics as dental material. *China Ceram.* **2005**, *41*, 17–20. (In Chinese)
21. Cheng, J.S.; Wu, G.Y.; He, F. Introduction of the new glass-ceramic/metal composite decorative materials. *Foshan Ceram.* **2014**, *14*, 40–41. (In Chinese)
22. Tian, P.; Liu, X.N.; Li, Z.X.; Guo, H.W.; He, Z. Research progress of oxidation-resistant glass-ceramic coatings on titanium alloys. *China Ceram.* **2010**, *46*, 3–6. (In Chinese)
23. Zhao, Y.C.; Liu, X.M. Development of Glass-ceramic Composites Research. *Mater. Mech. Eng.* **2007**, *31*, 10–12. (In Chinese)
24. Tao, Y.; Ma, Z.; Sun, F.H.; Li, L.Y.; Li, Z.C. Microstructure and Abrasive Resistance of Glass-Ceramic Composite Coatings from Fly Ash and Al-TiO<sub>2</sub>-B<sub>2</sub>O<sub>3</sub>. *Mater. Mech. Eng.* **2014**, *38*, 29–33. (In Chinese)
25. Yan, C.J. *Preparation and Properties of Glass Ceramic Composite Coating from Fly Ash*; Liaoning Technical University: Fuxin, China, 2012. (In Chinese)
26. Tee, K.L.; Lu, L.; Lai, M.O. In situ stir cast Al-TiB<sub>2</sub> composite: Processing and mechanical properties. *Mater. Sci. Technol.* **2001**, *17*, 201–206. [[CrossRef](#)]
27. Lakshmi, S.; Lu, L.; Gupta, M. In situ preparation of TiB<sub>2</sub> reinforced Al based composites. *J. Mater. Process. Technol.* **1998**, *73*, 160–166. [[CrossRef](#)]
28. Zhang, Q.; He, Y. Thermal shock resistance of cordierite glass-ceramics from fly ash. *China Ceram.* **2008**, *44*, 39–42. (In Chinese)
29. Ghosh, S. Thermal properties of glass-ceramic bonded thermal barrier coating system. *Trans. Nonferr. Met. Soc.* **2015**, *25*, 457–464. [[CrossRef](#)]
30. Harsha, S.; Dwivedi, D.K.; Agarwal, A. Influence of CrC addition in Ni-Cr-Si-B flame sprayed coatings on micro-structure, micro-hardness and wear behavior. *Int. J. Adv. Manuf. Technol.* **2008**, *38*, 93–101. [[CrossRef](#)]
31. An, Y.L.; Chen, J.M.; Zhou, H.D.; Wei, J.J. Preparation and Microstructure of Mullite SiO<sub>2</sub> Composite Coating. *Surf. Technol.* **2010**, *39*, 1–3. (In Chinese)
32. Xu, S.Q.; Hao, S.J.; Cao, B.G. Study for the effect factor of carbon dioxide corrosion rate on the oil and gas pipes. *Oil Field Equip.* **2007**, *36*, 44–46. (In Chinese)

